

УДК 616.711-001.5-073.763.5(045)

DOI: <http://dx.doi.org/10.15674/0030-59872026143-52>

## Radiographic morphometric prediction of new vertebral compression fractures after vertebroplasty

A. I. Popov<sup>1</sup>, M. V. Moloduk<sup>1</sup>, V. O. Kutsenko<sup>1</sup>, R. V. Zlatnik<sup>1</sup>, M. M. Nessonova<sup>2</sup>

<sup>1</sup>Sytenko Institute of Spine and Joint Pathology National Academy of Medical Sciences of Ukraine, Kharkiv

<sup>2</sup>Private higher educational institution «Kharkiv International Medical University». Ukraine

*New vertebral compression fractures (NVCF) following percutaneous vertebroplasty (PVP) remain a clinical challenge. Methods. A retrospective cohort study (2023–2025) was conducted at the Institute of Spine and Joint Pathology, Ukraine, involving 26 patients (24 females, 2 males; mean age  $(69.04 \pm 2.04)$  years) with osteoporotic vertebral compression fractures treated with PVP. Morphometric parameters of 99 vertebrae were assessed on digital radiographs (frontal/sagittal, RadiAnt DICOM Viewer, precision 0.1 mm / 0.1°): anterior ( $h_a$ ), middle ( $h_m$ ), posterior ( $h_p$ ) heights, relative compression (%), wedge index, local kyphotic angle, thoracic kyphosis, lumbar lordosis, and scoliosis. Results. NVCF occurred in 46.2 % of cases (45 fractures in 12 patients). Significant differences between NVCF and non-NVCF groups were observed for  $h_a$  compression ( $20.69 \pm 1.16$  mm vs.  $23.89 \pm 0.78$  mm,  $p = 0.0338$ ),  $h_m$  ( $17.84 \pm 1$  mm vs.  $21.31 \pm 0.61$  mm,  $p = 0.0021$ ),  $h_p$  ( $26.97 \pm 0.81$  mm vs.  $29.61 \pm 0.51$  mm,  $p = 0.0073$ ), lumbar lordosis ( $44.4^\circ \pm 1.52^\circ$  vs.  $38.28^\circ \pm 1.46^\circ$ ,  $p = 0.01$ ), and scoliosis ( $7.53^\circ \pm 0.56^\circ$  vs.  $5.90^\circ \pm 0.48^\circ$ ,  $p = 0.022$ ). The linear discriminant functions model, based on  $h_m$  (canonical correlation =  $-0.863$ ) and relative  $H_a$  compression (canonical correlation =  $0.139$ ), achieved Wilks'  $\Lambda = 0.8$  ( $\chi^2 = 15.77$ ,  $p = 0.000376$ ), classification accuracy of 76.25 % (sensitivity 76.9 %, specificity 75.9 %), and AUC =  $0.754 \pm 0.058$ . Adjusted function:  $F = 6.07 - 0.28 \times h_m$  (mm)  $- 0.035 \times H_a$  (%);  $F > 0$  indicates NVCF risk. Other parameters were excluded due to low discriminatory power or collinearity. Conclusion. This two-parameter model, using  $h_m$  and relative  $H_a$  compression, offers moderate predictive accuracy for NVCF post-PVP. Its simplicity suits resource-limited Ukrainian clinics. External validation and inclusion of confounders (e. g., BMD, therapy) are required for broader adoption.*

*Нові компресійні переломи хребців (НКПХ) після пункційної вертебропластики (ПВП) є серйозною проблемою вертебрології. Методи. У ретроспективне когортне дослідження (2022–2023 р.) включено 26 пацієнтів (24 жінки, 2 чоловіки; середній вік  $(69,04 \pm 2,04)$  роки) з остеопоротичними компресійними переломами хребців, яким виконувалася ПВП. Вивчено морфометричні параметри 99 хребців на цифрових рентгенограмах: висоти  $h_a$  (передня),  $h_m$  (середня),  $h_p$  (задня), відносна компресія  $H_a$ ,  $H_m$ ,  $H_p$  (%), ІК, локальний кіфотичний кут, грудний кіфоз, поперековий лордоз, сколіоз. Результати. Частота НКПХ склала 46,2 % (45 переломів у 12 пацієнтів). Значущі відмінності між групами з/без НКПХ виявлено для висоти  $h_a$  ( $20,69 \pm 1,16$  проти  $(23,89 \pm 0,78)$  мм,  $p = 0,0338$ ),  $h_m$  ( $17,84 \pm 1$  проти  $(21,31 \pm 0,61)$  мм,  $p = 0,0021$ ),  $h_p$  ( $26,97 \pm 0,81$  проти  $(29,61 \pm 0,51)$  мм,  $p = 0,0073$ ), поперекового лордозу ( $44,4^\circ \pm 1,52^\circ$  проти  $38,28^\circ \pm 1,46^\circ$ ,  $p = 0,01$ ) та сколіозу ( $7,53^\circ \pm 0,56^\circ$  проти  $5,90^\circ \pm 0,48^\circ$ ,  $p = 0,022$ ). Дискримінантна модель, яка базується на  $h_m$  (канонічна кореляція =  $-0,863$ ) та відносній компресії  $H_a$  (канонічна кореляція =  $0,139$ ), мала  $\Lambda$  Уїлкса =  $0,8$  ( $\chi^2 = 15,77$ ,  $p = 0,000376$ ), точність класифікації 76,25 % (чутливість 76,9 %, специфічність 75,9 %), AUC =  $0,754 \pm 0,058$ . Спроцена функція:  $F = 6,07 - 0,28 \times h_m$  (мм)  $- 0,035 \times H_a$  (%);  $F > 0$  свідчить про ризик НКПХ. Інші параметри виключено через низьку дискримінаційну цінність або колінеарність. Розроблено веб застосунок для прогнозування НКПХ. Висновки. Двопараметрична модель на основі висоти  $h_m$  та відносної компресії  $H_a$  забезпечує помірну прогностичну точність для виявлення ризику НКПХ після ПВП. Простота моделі робить її придатною для клінік із обмеженими ресурсами. Для впровадження потрібна зовнішня валідація та врахування додаткових чинників (мінеральна щільність кісткової тканини, терапія). Ключові слова. Пункційна вертебропластика, нові компресійні переломи, рентгеноморфометрія, дискримінантний аналіз, остеопороз.*

**Keywords.** Percutaneous vertebroplasty, new vertebral compression fractures, radiographic morphometry, discriminant functions analysis, osteoporosis

## Introduction

Percutaneous vertebroplasty (PVP) is the gold standard for minimally invasive treatment of osteoporotic vertebral compression fractures (VCFs), providing rapid pain relief, stabilization of the affected segment, and early restoration of functional activity in patients [1]. According to data from the U.S. and European registries, more than 300,000 PVP procedures are performed annually, with clinical effectiveness reaching 85-95% in the short term [2, 3].

However, the long-term outcomes of PVP are complicated by the development of new compression fractures (NCFs), which poses a significant clinical problem in modern vertebrology. Recent data from 2024-2025 shows that the frequency of symptomatic re-interventions after PVP ranges from 14.6 % to 22.2 % within 1-2 years of follow-up [4, 5]. A large cohort study of over 30,000 patients demonstrated that 15.5 % of cases required re-intervention within 24 months after the primary PVP procedure [4].

Radiomorphometric analysis remains the foundational method for assessing radiomorphometric parameters (RMP) of vertebrae and the degree of compression. Classical parameters proposed by H.K. Genant et al. include absolute and relative compression, wedge index, and the ratio of the anterior and posterior heights of the vertebrae [5]. The advantages of this approach include accessibility for hospitals with limited resources and the standardization of measurements [6].

Modern automated morphometric analysis systems based on artificial intelligence allow for the generalization of measurements and reduce inter-operator variability to less than 5% [7]. Y. Yang and colleagues demonstrated that MRI texture analysis combined with morphometric parameters achieves an AUC  $\approx$  0.80 for predicting the risk of fractures in patients with osteoporosis [8].

Multivariate discriminant analysis (MDA) is a classical statistical method for classification and prediction, widely used in medical research. Unlike complex machine learning algorithms, it provides transparency in mathematical calculations and ease of interpretation of results [9]. This method is especially effective when working with small samples and a limited number of parameters, making it useful in clinical practice [10].

Despite progress in the development of prognostic models for NCFs, most existing approaches are complex and require significant resources for implementation. It is important to note that there is little information regarding research on Ukrainian patients.

The development of a simple yet effective predictive model based on RMP that can be easily integrated into routine clinical practice in Ukrainian medical institutions is a relevant task.

*Purpose.* To identify the prognostic radiomorphometric parameters of vertebrae after percutaneous vertebroplasty that may be associated with the risk of developing new vertebral compression fractures and to develop a model for predicting these fractures.

## Materials and methods

The study was reviewed and approved by the Ethics and Deontology Committee of the Professor M. I. Sytenko Institute of Spine and Joint Pathology of the National Academy of Medical Sciences of Ukraine (protocol No. 260 dated 23.02.2026). All patients provided written consent for examination, treatment, and the use of medical data for scientific research.

This was a retrospective cohort study conducted at the Vertebrology Department of the Professor M. I. Sytenko Institute of Spine and Joint Pathology of the National Academy of Medical Sciences of Ukraine, from 2022 to 2023. The sample size consisted of 26 patients (24 women, 2 men; mean age  $(69.04 \pm 2.04)$  years, range 46–85) who underwent PVP due to VCFs as a result of osteoporosis. The diagnosis of “osteoporosis” was confirmed using dual-energy X-ray absorptiometry on the bone densitometer Explorer QDR W. The average follow-up period was 12 months, with NCFs diagnosed during follow-up visits at 1, 3, 6, and 12 months after PVP. In the studied cohort, 12 ( $46.2 \pm 9.8$ ) % of cases were verified with a total of 45 NCFs in the thoracic and lumbar regions of the spine.

Radiomorphometric parameters (RMP) of 99 treated vertebrae in the thoracic and lumbar spine were studied. Inclusion criteria: patients who underwent PVP for VCFs due to osteoporosis. Exclusion criteria: PVP due to malignant or traumatic fractures.

In a previous publication, we established that low bone mineral density (BMD), lack of anti-osteoporotic therapy, and advanced age increased the risk of developing NCFs by two times, and cement leakage almost tripled the risk [11]. Given this, these factors were not included in the study.

### *Radiomorphometric study*

The analysis of RMP was based on digital radiographs of the thoracic and lumbar spine obtained in two standard projections: frontal and sagittal. Radiographs were taken in a standing position (or lying down for patients with limited mobility). Radiographs

were obtained at three stages: before PVP, immediately after the procedure, and during follow-up visits (1, 3, 6, and 12 months). Only radiographs after PVP were included in the analysis. The image resolution met clinical standards (0.1–0.2 mm/pixel), ensuring the accuracy of measurements.

Image quality criteria: clear visualization of the endplate contours; symmetrical depiction of spinous processes (deviation < 5 mm); absence of rib overlap artifacts on vertebral bodies and motion artifacts; contrast allowing differentiation of cortical and trabecular bone structures.

RMP measurements were performed using RadiAnt DICOM Viewer software (version 2023.1), which allowed for linear and angular measurements with an accuracy of up to 0.1 mm and 0.1°. Below is a detailed description of the measured parameters.

**Vertebral height** ( $h_a$ ,  $h_m$ ,  $h_p$ ). Measurements were performed on both the vertebrae after PVP and the intact ones. The latter were used as reference values for calculating the percentage of compression according to the method of H. K. Genant et al., which allowed standardization of measurements across patients [5].

The upper and lower endplates of the vertebra were identified on the sagittal radiograph. Heights were measured as vertical distances between the corresponding points:

- $h_a$  (anterior height) — from the anterior edge of the cranial endplate to the anterior edge of the caudal endplate;
- $h_m$  (middle height) — in the middle of the vertebra (medial part);
- $h_p$  (posterior height) — from the posterior edge of the cranial endplate to the posterior edge of the caudal endplate.

To normalize the height, it was compared with the corresponding values of the neighboring intact vertebra.

**Relative compression** (%) was determined as the percentage of height loss relative to the reference.

$$H_a(\%) = \left( \frac{h_{a(\text{сусіднього})} - h_{a(\text{ушкодженого})}}{h_{a(\text{сусіднього})}} \right) \times 100, \quad (1)$$

For example, the relative compression of  $h_a$  was calculated using the formula (1): where  $h_a(\text{neighboring})$  — anterior height of the intact vertebra body (mm);  $h_a(\text{injured})$  — anterior height of the vertebral body after PVP (mm).

Similarly, the percentage of relative compression was determined for  $H_m$  and  $H_p$ .

**Wedge index** (WI) (%). To determine the wedge shape of the vertebrae, radiographs in the sagittal

$$IK = \frac{h_a}{h_p} \times 100. \quad (2)$$

projection were used. The height  $h_a$  and  $h_p$  were measured. The WI was calculated using the formula (2):

The results are expressed as percentages, where  $WI < 80\%$  indicates a wedge-shaped deformation.

The *local kyphotic angle* was measured as the Cobb angle formed between the line perpendicular to the cranial endplate of the neighboring proximal vertebra and the line perpendicular to the caudal endplate of the neighboring distal vertebra on the sagittal radiograph.

*Thoracic kyphosis* was evaluated as the Cobb angle between the cranial endplate of  $T_{IV}$  and the caudal endplate of  $T_{XII}$  on the sagittal projection.

*Lumbar lordosis* was measured between the cranial endplate of  $L_I$  and the caudal endplate of  $L_V$ .

*Scoliosis* was defined as the Cobb angle between the perpendicular lines to the cranial and caudal endplates of the most tilted vertebrae in the curve on the frontal projection.

Statistical data analysis was performed using the Statistica 13 software. The Shapiro-Wilk test was used to check the normality of the distribution of the variables. For paired comparisons of groups, depending on the presence of a new fracture, the Mann-Whitney non-parametric test was applied. Differences were considered statistically significant at a significance level of  $p < 0.05$ .

DA was employed in the development of a mathematical model for predicting NCFs. The quality of the constructed model was evaluated using ROC analysis through the web tool easyROC 1.3.1.

For the practical application of the developed NCF prediction model, a web application “Fracture Risk Calculator” has been created. The application is implemented using HTML, CSS, and JavaScript technologies and is available as a standalone web page, which can be integrated into medical institutions' systems. The user interface includes fields for entering values of  $h_m$  and  $H_a$ , a button to calculate, and a section to display the results.

## Results

The study of the distribution law of indicators using the Shapiro-Wilk test showed that only half of them were correct. Since the most clinically significant data, such as WI, as well as  $h_a$ ,  $h_m$ , and  $h_p$ , had a normal distribution, for descriptive statistics, in addition to medians (Me) and interquartile intervals ([LQ; UQ]), mean values (M) and standard errors of the means (m) were also used (Table 1).

Statistically significant differences between groups were observed only for the vertebral height indicators, which were higher in the group without NCF, and for the Cobb angles, which were used to assess scoliosis and lumbar lordosis. In patients with NCF, significantly higher angles of scoliosis and lumbar lordosis were recorded compared to those without NCF (Table 1, Figure 1).

During the construction of the NCF prediction model, RMP data after PVP for 80 observations were considered. The development of the NCF prediction

model was carried out using DA. Since there were only two groups in the data (NCF present/absent), DA was reduced to obtaining a single discriminant function (DF) and two classification functions (CF).

All 12 indicators after PVP were selected for analysis. Then, through stepwise removal (Backward stepwise), only significant indicators for classification were retained. As a result, only two values — vertebral height  $h_m$  and relative compression  $H_a$  — showed a statistically significant contribution to classifying the groups with or without NCF. The remaining

Table 1

Descriptive statistics for the compared groups with and without new compression fractures

Indicator	NCFs						p (Mann-Whitney test)
	absent			present			
	n	Me [LQ; UQ]	M ± m	n	Me [LQ; UQ]	M ± m	
1	2	3	4	5	6	7	8
Age, years	14	67.5 [59.0; 76.0]	67.7 ± 3.2	12	74.0 [63.0; 78.5]	70.60 ± 2.50	0.462000
Thoracic kyphosis, degrees	21	52.50 [26.20; 64.00]	44.62 ± 5.01	21	45.00 [44.90; 56.00]	50.00 ± 3.02	0.900980
*Lumbar lordosis, degrees	33	38.70 [34.90; 43.20]	38.28 ± 1.46	40	43.00 [40.00; 45.30]	44.4 ± 1.52	0.009467
*Scoliosis, degrees (all data)	49	5.50 [2.90; 7.40]	5.90 ± 0.48	41	7.50 [5.50; 10.70]	7.53 ± 0.56	0.0219400
– thoracic spine,	21	5.30 [4.00; 6.00]	5.49 ± 0.60	23	7.00 [4.50; 8.60]	6.69 ± 0.71	0.111589
– lumbar spine,	28	5.75 [2.80; 8.40]	6.21 ± 0.70	18	9.10 [5.60; 12.70]	8.61 ± 0.85	0.073117
Local kyphotic angle, degrees (all data)	53	14.30 [8.90; 20.70]	14.71 ± 1.07	17	18.35 [8.80; 26.80]	18.00 ± 1.74	0.156685
– *thoracic spine,	22	16.20 [7.90; 19.30]	15.69 ± 1.76	22	20.50 [13.80; 27.10]	20.75 ± 1.86	0.035627
– lumbar spine,	31	13.60 [8.90; 20.70]	14.02 ± 1.35	18	12.25 [3.40; 25.90]	14.66 ± 3.01	0.787415
Wedge index, % (all data)	54	81.5 [69.0; 93.0]	80.5 ± 2.18	41	75.0 [62.0; 90.0]	74.98 ± 3.15	0.155460
– thoracic spine,	22	79.0 [67.0; 85.0]	76.55 ± 3.08	23	72.0 [59.0; 79.0]	69.00 ± 0.04	0.059404
– lumbar spine,	32	86.0 [69.5; 96.5]	83.22 ± 2.95	18	86.0 [72.0; 97.0]	82.61 ± 0.045	0.935539
*Height $h_a$ , mm (all data)	54	24.75 [19.00; 28.10]	23.89 ± 0.78	41	20.60 [16.50; 25.90]	20.69 ± 1.16	0.033767
– * $h_a$ (thoracic spine),	22	21.30 [17.90; 24.10]	21.00 ± 1.03	23	17.70 [15.30; 22.00]	17.31 ± 1.19	0.030085
– $h_a$ (lumbar spine),	32	27.20 [20.75; 29.85]	25.87 ± 0.98	18	26.10 [19.80; 30.70]	25.01 ± 1.72	0.959696
*Height $h_m$ , mm (all data)	54	21.35 [17.90; 24.50]	21.31 ± 0.61	41	17.90 [13.80; 21.40]	17.84 ± 0.99	0.002063
– $h_m$ (thoracic spine),	22	18.50 [17.30; 21.60]	18.97 ± 0.87	23	17.40 [13.30; 19.10]	15.67 ± 0.99	0.035650
– $h_m$ (lumbar spine),	32	22.65 [20.35; 25.35]	22.92 ± 0.71	18	20.80 [15.20; 25.20]	20.62 ± 1.67	0.959696

Continuation of table 1

1	2	3	4	5	6	7	8
*Height $h_p$ , mm (all data)	54	30.50 [27.60; 32.30]	$29.61 \pm 0.51$	41	27.70 [23.00;30.60]	$26.97 \pm 0.81$	0.007302
– $h_p$ (thoracic spine),	22	28.20 [24.60; 29.90]	$27.33 \pm 0.70$	23	24.40 [21.80;28.00]	$24.77 \pm 1.05$	0.044426
– $h_p$ (lumbar spine),	32	31.50 [30.25; 33.35]	$31.175 \pm 0.58$	18	30.00 [28.10;31.30]	$29.78 \pm 0.93$	0.101509
Relative compression $H_a$ , % (all data)	54	14.13 [5.00; 27.83]	$17.46 \pm 2.34$	28	20.64 [7.65;35.48]	$26.18 \pm 5.55$	0.275572
– $H_a$ (thoracic spine),	22	6.96 [2.17; 23.75]	$11.59 \pm 3.69$	20	20.64 [5.68;29.09]	$22.38 \pm 6.10$	0.186093
– $H_a$ (lumbar spine),	32	15.54 [11.09; 33.05]	$21.49 \pm 2.85$	8	23.98 [10.43;54.78]	$35.67 \pm 12.09$	0.576908
Relative compression $H_m$ , % (all data)	54	30.00 [20.83; 41.32]	$30.91 \pm 1.96$	28	35.38 [26.74;50.84]	$40.72 \pm 4.52$	0.105574
– $H_m$ (thoracic spine),	22	25.625 [18.85; 44.17]	$27.56 \pm 3.48$	20	34.32 [28.03;46.66]	$37.40 \pm 5.04$	0.137297
– $H_m$ (lumbar spine),	32	34.08 [25.07; 40.80]	$33.21 \pm 2.25$	8	44.91 [25.72;63.16]	$49.03 \pm 9.48$	0.170852
Relative compression $H_p$ , % (all data)	54	9.37 [4.78; 18.42]	$11.75 \pm 1.26$	28	7.04 [3.27;17.28]	$16.65 \pm 4.86$	0.567286
– $H_p$ (thoracic spine),	22	6.49 [2.11; 9.60]	$7.05 \pm 1.44$	20	4.91 [2.35;13.86]	$11.98 \pm 4.94$	0.969866
– $H_p$ (lumbar spine),	32	15.78 [7.12; 20.27]	$14.99 \pm 1.68$	8	19.095 [7.22;35.15]	$28.30 \pm 11.20$	0.370213

Notes: n — number of observations (age data, vertebral fractures in relation to other indicators); \* — statistically significant differences between groups depending on the presence of NCFs.

indicators were excluded from the model due to insufficient discriminatory ability, which may be caused, for example, by either the lack of significant variability of the indicator between groups or a high level of correlation with other variables.

When evaluating the statistical significance of the obtained DF using the approximation of the distribution by the  $\chi^2$  function from the Wilks'  $\Lambda$ -statistic, a p-value of 0.000376 was obtained for  $\Lambda = 0.8$  and  $\chi^2 = 15.77$ , indicating its significance.

The contribution of each of the two indicators to the classification can be judged by the magnitude of the factor structure coefficients (Table 2): the largest is  $h_m$ , with a canonical correlation between the indicator and DF of  $-0.863$ .

For classifying observations into groups (NCF present/absent after PVP), the following CFs were obtained:

$$F_{\text{absent}} = -23.22 + 1.83 \times h_m + 0.32 \times H_a, \quad (3)$$

$$F_{\text{present}} = -17.05 + 1.55 \times h_m + 0.28 \times H_a. \quad (4)$$

According to the classical scheme of using DA models, observations are assigned to the group for

which the larger value of CF is obtained. However, in the case of only two classes, it is obviously more appropriate to consider the difference between the two CFs.

In our case:

$$\Delta F = F_{\text{present}} - F_{\text{absent}} = 6.17 - 0.28 \times h_m - 0.035 \times H_a. \quad (5)$$

If  $\Delta F$  is greater than 0, a new compression fracture is likely to occur; if  $\Delta F$  is less than 0, it is unlikely to happen. The results of the posterior classification (Table 3) indicate a fairly good adequacy of the developed model, which is also confirmed by the corresponding estimates of the area under its ROC curve:  $AUC = 0.754$  with a 95 % CI ranging from 0.640 to 0.867 (Figure 2).

The optimal threshold value obtained from the ROC analysis for the developed model allowed increasing the overall accuracy of prediction from 73.75 % to 76.25 %, by increasing its specificity (accuracy of determining the absence of a new compression fracture) to 75.9 % (95 % CI from 62.4 to 86.5 %), without changing the sufficiently high sensitivity, which remained at 76.9 % with a 95 % CI from 56.4 to 91.0 % (Figure 2). Therefore, the formula for



Fig. 1. Box plots of some indicators after PVP (NCF)

**Factor structure coefficients for the built discriminant analysis model of predicting NCFs**

Indicator	Canonical correlation between the indicator and DF
Height $h_m$ , MM	-0.863
Relative compression $H_a$ , %	0.139

predicting a new compression fracture, adjusted for the optimal cutoff threshold, looks as follows:

$$\Delta F = 6.07 - 0.28 \times h_m - 0.035 \times H_a. \quad (6)$$

As before, the absence of an NCPF corresponds to  $\Delta F < 0$ , and its presence corresponds to  $\Delta F > 0$ .

Since in our study only two groups were classified using two explanatory variables, it is quite easy to visualize the discrimination of observations on a two-dimensional scatter plot (Figure 3), where the line corresponds to the discriminant function.

The developed web application “Fracture Risk Calculator” successfully implements the discriminant model for predicting NCPF using the RMPs  $h_m$

Table 2

and  $H_a$  (Figure 4). Testing the application on a sample of 80 observations showed that it correctly reproduces the results of the discriminant analysis, providing a classification accuracy of 76.25 %. A  $\Delta F > 0$  indicates the risk of NCPF, while  $\Delta F \leq 0$  indicates its absence.

### Discussion

This study is the first attempt to develop a predictive model for the risk of NCPF after PVF in the Ukrainian population based on RMPs. The obtained results demonstrate both the potential and the limitations of the simplified two-parameter approach to predicting NCPF.

Within the conducted analysis, statistically significant differences in the RMPs of vertebrae after PVF were found between patients with and without the development of NCPF. At the same time, it is crucial to emphasize that morphometric characteristics are not the direct cause of new compression fractures of the vertebrae; they reflect the systemic properties of the bone tissue and the biomechanical state of the spine, which determine the individual risk

Table 3

Posterior classification matrix for the DF model for predicting NCFs

Studies sample	Percentage of the correct ( %)	Predicted by the model (n)	
		NCF absent	NCF present
NCF absent (n = 54)	72.20	39	15
NCF present (n = 26)	76.90	6	20
Total (n = 80)	73.75	47	33

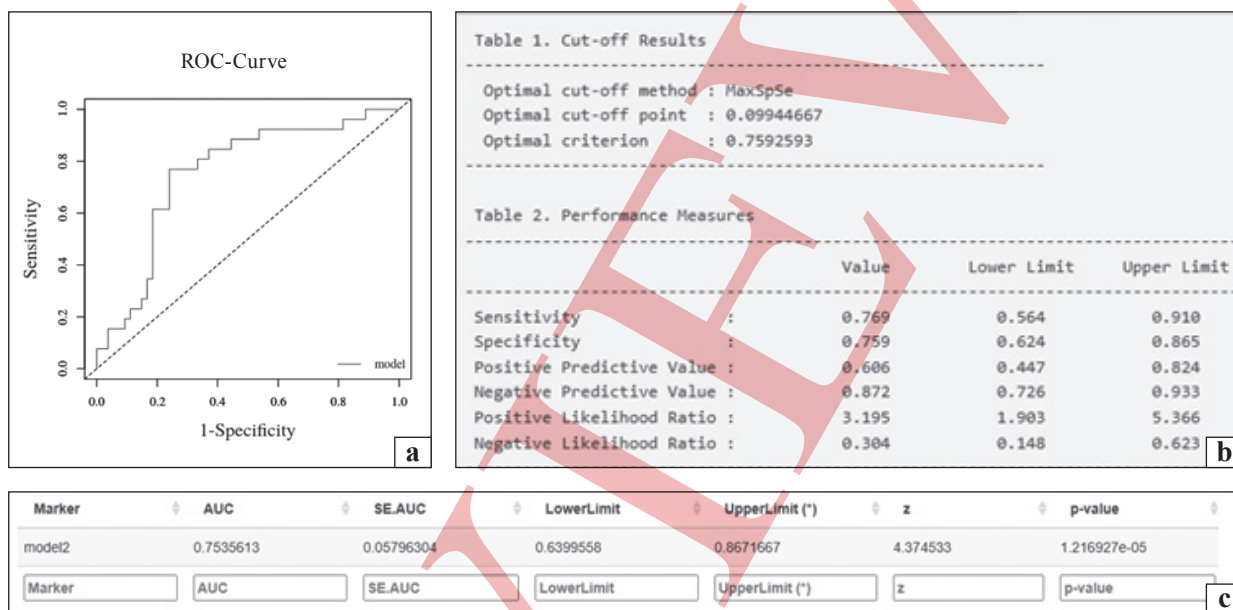


Fig. 2. Results of ROC analysis for the developed DF model for predicting NCF: (a) ROC curve plot; (b) results of determining the optimal cutoff threshold; (c) area under the ROC curve evaluations.

of new compression fractures. In essence, this concept is analogous to the use of the BMD indicator, which itself does not “cause” fractures but serves as a reliable marker of the risk of their occurrence by reflecting the quality of bone tissue.

This position is supported by numerous experimental and clinical studies.

Thus, H. K. Genant et al. demonstrated a strong negative correlation between the degree of vertebral body compression and BMD ( $r = -0.68$ ;  $p < 0.001$ ) [5]. In turn, S. Boutrouy et al. using quantitative computed tomography showed that in patients with compression over 40 %, the volumetric density of trabecular bone is 35 % lower, and the cortical layer porosity is 28 % higher compared to those with compression less than 25 % [12]. Therefore, pronounced vertebral deformity is a marker of more severe systemic osteoporosis and poorer bone quality not only in the affected segment but also throughout the spine, which pathophysiologically justifies the increased susceptibility of such patients to the development of NCPFs.

Beyond systemic factors, local biomechanical alterations following PVP are also significant contrib-

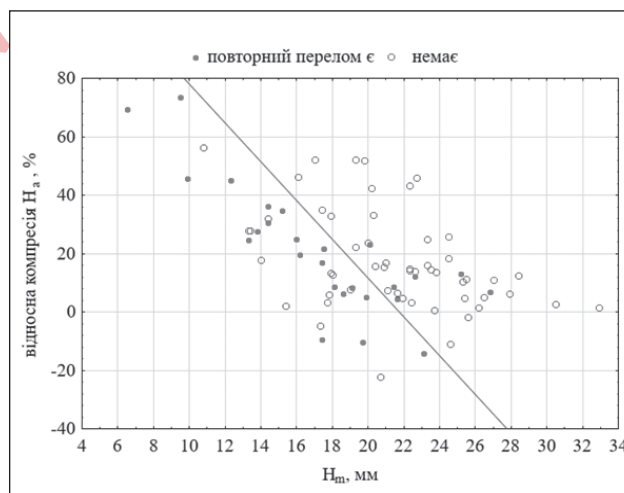
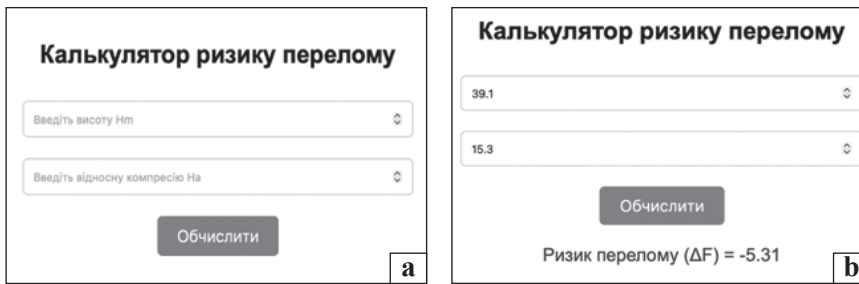


Fig. 3. Scatter plot of the indicators  $h^m$  and relative compression  $H_a$ .

utors. Specifically, J. Luo et al. in a study using finite element analysis showed that after PVP of vertebrae with compression over 33 %, the load on adjacent segments increases by 18–24 %, while with compression less than 25 %, it increases only by 8–12 % [13]. Clinical observations are consistent with these data.



**Fig. 4.** Web application “Fracture Risk Calculator”: (a) interface; (b) results of the work

R. Lindsay et al. found that compression over 40 % is associated with a 92 % increase in the risk of NCPF within one year, while for compression less than 25–38 %, the increase is 45 % [14]. In a long-term prospective study by J. A. Cauley et al. (15 years,  $n = 9,704$ ), it was shown that the degree of vertebral deformity is an independent risk factor for NCPF ( $HR = 2.8$ ; 95 % CI: 1.9–4.2) [15].

The results obtained in our study are consistent with the above data and suggest that the morphometric parameters  $hm$  and  $Ha$  can be considered accessible markers for identifying the risk of NCPF after PVP in clinical practice. At the same time, it should be noted that the frequency of NCPF in our sample (46.2 %) significantly exceeds the values reported in most current publications. A meta-analysis by A. J. Láinez Ramos-Bossini et al., which included 14 randomized controlled trials ( $n = 1,413$ ), did not find a statistically significant increase in the risk of NCPF after vertebroplasty compared to conservative treatment ( $RR = 1.05$ ) [16]. However, in the Optum cohort study of individuals after PVP, the frequency of new interventions was shown to be 15.5 % over 24 months of observation [4]. The observed discrepancies are likely due to the specific patient selection criteria in our study, which is confirmed by previous data: in a cohort of 520 patients who underwent PVP, the frequency of NCPF was 12.31 % [17].

The last decade has been characterized by intensive development of predictive models for individual risk assessment of NCPF. Traditional statistical approaches include multifactorial regression models and nomograms. For example, Q. Li et al. proposed a 12-parameter nomogram that integrates clinical, radiological, and technical variables, with an area under the ROC curve (AUC) of 0.85 [18]. Y. Qian et al. developed a simplified 8-parameter model with an AUC of 0.83, but even such tools remain relatively complex for routine clinical use [19].

The further development of this direction is linked to the implementation of artificial intelligence (AI) and machine learning methods. H. Wu et al. demonstrated that the support vector machine method pro-

vides the highest accuracy in predicting NCPF after PVP among the compared algorithms based on a sample of 863 patients [20]. S. Kim et al. applied a Vision Transformer-based model for analyzing MRI images, achieving a statistically significant improvement in AUC compared to classical neural networks [21]. Y. Yeh et al. demonstrated the high predictive value of the Vertebral Bone Quality Score (VBQ) as a predictor of NCPF (AUC = 0.74) [22].

Our model achieved an accuracy of 76.25 %, which corresponds to moderate discriminatory ability by the criteria of J. A. Swets [23]. Although these figures are lower than those of more complex multi-parameter and AI-based models [20–22], they are comparable to the results of simpler statistical approaches presented in the literature.

The key advantage of the proposed model is its practical applicability. The use of only two variables, which can be measured using standard radiography, makes this tool potentially suitable for widespread implementation, especially in the context of limited resources in Ukraine's healthcare system.

The statistical significance of the  $Ha$  and  $hm$  parameters has a clear biomechanical basis. For example, C. Zhou et al., in studies using the finite element method, showed that vertebrae with an initial compression of the anterior vertebral edge exceeding 25 % have 35–45 % higher stress in adjacent segments after the introduction of bone cement [24]. The mean value of  $Ha$  in the group of patients with NCPF in our study (20.64) is consistent with these data. The reduction in the absolute height of the anterior vertebral edge ( $> 17.2$  mm) reflects not only the degree of local compression but also its overall architectural degradation. In this context, it is noteworthy that Y. Yeh et al. demonstrated the independent prognostic value of the Vertebral Bone Quality Score, which correlates with morphometric parameters (MP), regarding the risk of NCPF [22].

An important point is that a systematic review by S. R. Namireddy et al. showed that simpler statistical models often demonstrate better generalizability compared to complex artificial intelligence algo-

gorithms in the context of external validation [25]. This emphasizes the appropriateness of developing simple, interpretable, and reproducible tools for routine clinical practice.

Thus, at the present stage, the proposed model can be considered a promising auxiliary tool for the primary assessment of the risk of NCPF after PVP. However, it requires further refinement and external validation before being implemented in widespread clinical practice.

## Conclusion

The developed model for predicting new compression fractures of the vertebrae after percutaneous vertebroplasty is promising and is based on the morphometric parameters of vertebral height (hm) and relative compression (Ha) after PVP. The model demonstrates moderate accuracy in posterior classification (76.25 %) and statistical significance ( $p = 0.000376$ ). The application of the model may aid in the early identification of patients at high risk for NCPF, allowing for the optimization of preventive strategies.

**Conflict of interest.** The authors declare no conflict of interest.

**Future research directions.** Future research should focus on the external validation of the developed model in other medical institutions and on independent patient cohorts, as well as its prospective clinical testing. Further work should aim at enhancing the model by integrating additional clinical and instrumental indicators.

**Funding information.** The study was conducted within the framework of the planned scientific research at the State Institution Professor M. I. Sytenko Institute of Spine and Joint Pathology of the National Academy of Medical Sciences of Ukraine. No additional funding was received.

**Authors' contribution.** Popov A. I. — study concept, patient treatment, article editing; Molodyuk M. V. — data collection, drafting the article, patient treatment; Kutsenko V. O. — study concept, literature review, drafting the article; Zlatnik R. V. — radiological diagnosis, morphometric measurements; Nessonova M. M. — statistical analysis, interpretation of findings, article editing.

## References

- Rho, Y., Choe, W. J., & Chun, Y. I. (2011). Risk factors predicting the new symptomatic vertebral compression fractures after percutaneous vertebroplasty or kyphoplasty. *European Spine Journal*, 21(5), 905–911. <https://doi.org/10.1007/s00586-011-2099-5>
- Sahota, A., Vass, C., Marshall, L., & Sahota, O. (2024). Fragility fracture and fear of falling in middle aged adults—a prevalence study. *Osteoporosis International*, 35(12), 2237–2238. <https://doi.org/10.1007/s00198-024-07166-6>
- Hernlund, E., Svedbom, A., Ivergård, M., Compston, J., Cooper, C., Stenmark, J., McCloskey, E. V., Jönsson, B., & Kanis, J. A. (2013). Osteoporosis in the European Union: Medical management, epidemiology and economic burden. *Archives of Osteoporosis*, 8(1–2). <https://doi.org/10.1007/s11657-013-0136-1>
- Hirsch, J. A., Gilligan, C., Chandra, R. V., Brook, A., Gasquet, N. C., Ricker, C. N., & Wu, C. (2024). Real-world rates and risk factors for subsequent treatment with vertebroplasty or balloon kyphoplasty after initial vertebral augmentation: A retrospective cohort study. *Osteoporosis International*, 36(1), 129–140. <https://doi.org/10.1007/s00198-024-07294-z>
- Genant, H. K., Wu, C. Y., Van Kuijk, C., & Nevitt, M. C. (1993). Vertebral fracture assessment using a semiquantitative technique. *Journal of Bone and Mineral Research*, 8(9), 1137–1148. <https://doi.org/10.1002/jbmr.5650080915>
- Kuo, C. (2024). Commentary on “Deep learning-assisted quantitative measurement of thoracolumbar fracture features on lateral radiographs”. *Neurospine*, 21(1), 44–45. <https://doi.org/10.14245/ns.2448202.101>
- Thrall, J. H. (2024). Challenges of implementing artificial intelligence-enabled programs in the clinical practice of radiology. *Radiology: Artificial Intelligence*, 6(5). <https://doi.org/10.1148/ryai.240411>
- Yang, Y., Peng, J., Deng, K., Zhang, Z., Qiu, Q., & Zhang, X. (n. d.). Prediction of vertebral fracture risk in patients with osteopenia based on MRI texture analysis. *ISMRM Annual Meeting*. <https://doi.org/10.58530/2024/1553>
- Tabachnick, B. G., & Fidell, L. S. (2019). *Using multivariate statistics* (7<sup>th</sup> ed.). Pearson.
- Izenman, A. J. (2013). *Modern multivariate statistical techniques*. Springer. <https://doi.org/10.1007/978-0-387-78189-1>
- Popov, A., Moloduk, M., Kutsenko, V., & Nessonova, M. (2025). Risk factors for recurrent vertebral compression fractures after percutaneous vertebroplasty in osteoporotic patients: A systematic review and meta-analysis. *ORTHOPAEDICS TRAUMATOLOGY and PROSTHETICS*, 3(3), 91–102. <https://doi.org/10.15674/0030-59872025391-102>
- Boutroy, S., Bouxsein, M. L., Munoz, F., & Delmas, P. D. (2005). In Vivo Assessment of Trabecular Bone Microarchitecture by High-Resolution Peripheral Quantitative Computed Tomography. *The Journal of Clinical Endocrinology & Metabolism*, 90(12), 6508–6515. <https://doi.org/10.1210/jc.2005-1258>
- Luo, J., Skrzypiec, D. M., Pollintine, P., Adams, M. A., Annesley-Williams, D. J., & Dolan, P. (2007). Mechanical efficacy of vertebroplasty: Influence of cement type, BMD, fracture severity, and disc degeneration. *Bone*, 40(4), 1110–1119. <https://doi.org/10.1016/j.bone.2006.11.021>
- Lindsay, R. (2001). Risk of New Vertebral Fracture in the Year Following a Fracture. *JAMA*, 285(3), 320. <https://doi.org/10.1001/jama.285.3.320>
- Cauley, J. A., Hochberg, M. C., Lui, L.-Y., Palermo, L., Ensrud, K. E., Hillier, T. A., Nevitt, M. C., & Cummings, S. R. (2007). Long-term Risk of Incident Vertebral Fractures. *JAMA*, 298(23), 2761. <https://doi.org/10.1001/jama.298.23.2761>
- Láinez Ramos-Bossini, A. J., Jiménez Gutiérrez, P. M., Moraleda Cabrera, B., Bueno Caravaca, L., González Díez, M., & Ruiz Santiago, F. (2024). Risk of new vertebral compression fractures and serious adverse effects after vertebroplasty: A systematic, critical review and meta-analysis of randomized controlled trials. *Quantitative Imaging in Medicine and Surgery*, 14(11), 7848–7861. <https://doi.org/10.21037/qims-24-396>
- Popov, A., & Moloduk, M. (2024). Prediction of repeated osteoporotic fractures of the thoracic and lumbar vertebrae (experimental study). *Orthopaedics, Traumatology and Prosthetics*, 3(3), 5–12. <https://doi.org/10.15674/0030-5987202435-12>
- Li, Q., Long, X., Wang, Y., Fang, X., Guo, D., Lv, J., Hu, X., & Cai, L. (2021). Development and validation of a nomogram for predicting the probability of new vertebral compression fractures after vertebral augmentation of osteoporotic vertebral compression fractures. *BMC Musculoskeletal Disorders*, 22(1). <https://doi.org/10.1186/s12891-021-04845-x>
- Qian, Y., Hu, X., Li, C., Zhao, J., Zhu, Y., Yu, Y., Xie, N., Ma, B., Zeng, Z., & Cheng, L. (2023). Development of a nomogram

- model for prediction of new adjacent vertebral compression fractures after vertebroplasty. *BMC Surgery*, 23(1). <https://doi.org/10.1186/s12893-023-02068-6>
20. Wu, H., Li, C., Song, J., & Zhou, J. (2024). Developing predictive models for residual back pain after percutaneous vertebral augmentation treatment for osteoporotic thoracolumbar compression fractures based on machine learning technique. *Journal of Orthopaedic Surgery and Research*, 19(1). <https://doi.org/10.1186/s13018-024-05271-0>
  21. Kim, S., Kim, I., Yuh, W. T., Han, S., Kim, C., Ko, Y. S., Cho, W., & Park, S. B. (2024). Augmented prediction of vertebral collapse after osteoporotic vertebral compression fractures through parameter-efficient fine-tuning of biomedical Foundation models. *Scientific Reports*, 14(1). <https://doi.org/10.1038/s41598-024-82902-w>
  22. Yeh, Y., Chen, M., Hu, Y., Chiu, P., Kao, F., Hsieh, M., Yu, C., Tsai, T., Niu, C., Chen, W., & Lai, P. (2024). Vertebral bone quality score as a predictor of subsequent fractures after cement augmentation for Osteoporotic vertebral compression fracture. *Neurosurgery*, 96(6), 1410–1418. <https://doi.org/10.1227/neu.0000000000003282>
  23. Swets, J. A. (1988). Measuring the accuracy of diagnostic systems. *Science*, 240(4857), 1285–1293. <https://doi.org/10.1126/science.3287615>
  24. Zhou, C., Meng, X., Huang, S., Chen, H., Zhou, H., Liao, Y., Tang, Z., Zhang, X., Li, H., Sun, W., & Wang, Y. (2024). Biomechanical study of different bone cement distribution on osteoporotic vertebral compression Fracture-A finite element analysis. *Heliyon*, 10(5), e26726. <https://doi.org/10.1016/j.heliyon.2024.e26726>
  25. Namireddy, S. R., Gill, S. S., Peerbhai, A., Kamath, A. G., Ramsay, D. S., Ponniah, H. S., Salih, A., Jankovic, D., Kalasauskas, D., Neuhoff, J., Kramer, A., Russo, S., & Thavarajasingam, S. G. (2024). Artificial intelligence in risk prediction and diagnosis of vertebral fractures. *Scientific Reports*, 14(1). <https://doi.org/10.1038/s41598-024-75628-2>

The article has been sent to the editors 21.10.2025	Received after review 28.11.2025	Accepted for printing 09.12.2025
--	-------------------------------------	-------------------------------------

## RADIOGRAPHIC MORPHOMETRIC PREDICTION OF NEW VERTEBRAL COMPRESSION FRACTURES AFTER VERTEBROPLASTY

A. I. Popov <sup>1</sup>, M. V. Moloduk <sup>1</sup>, V. O. Kutsenko <sup>1</sup>, R. V. Zlatnik <sup>1</sup>, M. M. Nessonova <sup>2</sup>

<sup>1</sup> Sytenko Institute of Spine and Joint Pathology National Academy of Medical Sciences of Ukraine, Kharkiv

<sup>2</sup> Private higher educational institution «Kharkiv International Medical University». Ukraine

- ✉ Andrii Popov, MD, DSci in Orthopaedics and Traumatology: [aipopovdoc@gmail.com](mailto:aipopovdoc@gmail.com); <https://orcid.org/0000-0002-9006-7721>
- ✉ Mykyta Moloduk, MD: [NikitaMoloduk@gmail.com](mailto:NikitaMoloduk@gmail.com); <https://orcid.org/0009-0005-0058-424X>
- ✉ Volodymyr Kutsenko, MD, DSci in Orthopaedics and Traumatology: [kutsvlad1956@gmail.com](mailto:kutsvlad1956@gmail.com); <https://orcid.org/0000-0001-7924-6553>
- ✉ Ruslan Zlatnik, MD: [ruslan.zlatnik@gmail.com](mailto:ruslan.zlatnik@gmail.com); <https://orcid.org/0009-0005-7621-9118>
- ✉ Maryna Nessonova, PhD in Technology: [m.nessonova@khimu.edu.ua](mailto:m.nessonova@khimu.edu.ua); <https://orcid.org/0000-0001-7729-317X>